

---

# Influence of $\text{Li}_2\text{CO}_3$ and ZnO Nanoparticle on Microstructure and Magnetic Properties of Low-Temperature Sintering LiZnTiBi Ferrites for High-Frequency Applications

Fang Xu<sup>\*</sup>, Yulong Liao, Huaiwu Zhang<sup>\*</sup>

State Key Laboratory of Electronic Thin Film and Integrated Devices, University of Electronic Science and Technology of China, Chengdu, China

## Email address:

fxu2331@gmail.com (Fang Xu), hwzhang@uestc.edu.cn (Huaiwu Zhang)

<sup>\*</sup>Corresponding author

## To cite this article:

Fang Xu, Yulong Liao, Huaiwu Zhang. Influence of  $\text{Li}_2\text{CO}_3$  and ZnO Nanoparticle on Microstructure and Magnetic Properties of Low-Temperature Sintering LiZnTiBi Ferrites for High-Frequency Applications. *International Journal of Materials Science and Applications*. Vol. 8, No. 3, 2019, pp. 35-39. doi: 10.11648/j.ijmsa.20190803.11

**Received:** May 28, 2019; **Accepted:** July 24, 2019; **Published:** July 29, 2019

---

**Abstract:** LiZnTi ferrite ceramics with high saturation flux density ( $B_s$ ), large remanence ratio ( $B_r/B_s$ ) and high saturation magnetization ( $4\pi M_s$ ) is a vital material for high frequency devices. In the present work, we prepared uniform and compact LiZnTiBi ferrite with large average grain size ( $>30\mu\text{m}$ ) at  $900^\circ\text{C}$ . Firstly, the hybrid materials, including  $\text{Li}_2\text{CO}_3$ , ZnO,  $\text{TiO}_2$ ,  $\text{Bi}_2\text{O}_3$  and  $\text{Fe}_2\text{O}_3$ , were pre-sintered at  $850^\circ\text{C}$  at  $\text{O}_2$  atmosphere. Next, composite additives composed of  $\text{Li}_2\text{CO}_3$  and ZnO nanoparticles were added to control grain growth. The influences of the  $\text{Li}_2\text{CO}_3$  and nano-ZnO (LZ) on the microstructure and magnetic properties of LiZnTiBi ferrite, especially for grain size, have been analyzed. SEM images demonstrated that moderate LZ additives ( $x=0.75$  wt%) can prevent abnormal grains. Also, the ferrite samples possess compact microstructures. The phenomenon indicated that the LZ additive is a good sintering aid for low-temperature sintering LiZnTiBi ferrites. XRD patterns showed that all samples have a pure spinel phase. The magnetic properties, including  $B_s$ ,  $B_r/B_s$  and  $4\pi M_s$ , have weak change when LZ additives were added. However, due to smaller average grain size, the coercivity ( $H_c$ ) gradually increased. Thus, a low-temperature sintering LiZnTiBi ferrite with high saturation flux density ( $B_s=311.10$  mT), large remanence ratio ( $B_r/B_s=0.86$ ), low coercivity ( $H_c=244.6$  A/m) and high saturation magnetization ( $M_s=75.40$ ) was obtained when 1.00 wt% LZ additive was added. More important, the LiZnTiBi ferrite possessed uniform average grain. Such a sintering method (i.e., adding composite additive to control abnormal grain) should also promote synthesis of other advanced ceramics for practical applications.

**Keywords:** LiZnTiBi Ferrite, Low Temperature Sintering,  $\text{Li}_2\text{CO}_3$ , ZnO Nanoparticle, Microstructure, Magnetic Properties

---

## 1. Introduction

Recent developments and progresses in low temperature co-fired ferrite (LTCC) are attracting widely interests for miniaturized and integrated microwave devices, such as antenna, phase shifter, circulator and filter [1-5]. For instance, as a vital passive device for phased array radar antenna, phase shifter has urgent requirement for miniaturization and integration [6]. Therefore, to develop miniaturized, high power capacity and high-frequency phase shifter, ferrite phase shifter has attracted more attentions from researchers in recent years [7]. Due to high resistivity and great magnetic

properties, ferrite ceramics with low sintering temperature have been widely studied, such as LiZn ferrite [8-11].

LiZn ferrite is a good and optional material for high-frequency microwave devices because of its high Curie temperature ( $T_c$ ), high remanence ratio ( $B_r/B_s$ ) and large saturation magnetization ( $4\pi M_s$ ) [12]. However, high sintering temperature of the LiZn ferrite don't meet requirement of low temperature co-fired ceramic (LTCC) technology. In addition, the high temperature can lead to Li element volatilization and cause composition segregation of the ferrite. Thus, lower sintering temperature of LiZn ferrite is vital for expanding application filed. However, when the

sintering temperature of the LiZn ferrite ceramics decreased to  $\sim 900^\circ\text{C}$ , insufficient grain growth and overmuch pores of the ferrite samples resulted in reduction of magnetic performances and increase of magnetic loss. In order to realize low temperature sintering, nanoparticle, low-melting point oxides or glasses are selected as sintering additives [13-14]. In our previous work,  $\text{Bi}_2\text{O}_3$  was proved to be a great additive, which can promote grain growth at  $\sim 920^\circ\text{C}$  because of reduction of activation energy [12]. Also, to obtain uniform and compact ferrite materials, various additives, such as LBSCA, BBSA glass and  $\text{V}_2\text{O}_5$ , have been widely studied in recent years [15-17]. However, overmuch additive was added, the magnetic properties of ferrite ceramics become worse.

Therefore, in the present work, to control grain growth and obtain great magnetic properties, low-melting-point  $\text{Li}_2\text{CO}_3$  and ZnO nanoparticle (LZ additive) are selected as fluxing agent of  $\text{Li}_{0.43}\text{Zn}_{0.27}\text{Ti}_{0.13}\text{Bi}_{0.003}\text{Fe}_{2.167}\text{O}_4$  (i.e., LiZnTiBi) ferrite ceramic with low sintering temperature ( $\sim 900^\circ\text{C}$ ). During the sintering process, the  $\text{Li}_2\text{CO}_3$  can offset Li loss. Importantly, the nano-ZnO particle can refine grain of the ferrite and control abnormal grains. In the work, the influences of the  $\text{Li}_2\text{CO}_3$  and ZnO nanoparticle composite additives on phase structure, microstructure, and magnetic properties of the LiZnTiBi ferrite sintered at low temperature have been discussed in detailed.

## 2. Main Body

### 2.1. Experimental Section

Firstly, raw materials, including  $\text{Li}_2\text{CO}_3$ , ZnO,  $\text{TiO}_2$ ,  $\text{Bi}_2\text{O}_3$  and  $\text{Fe}_2\text{O}_3$  (AR, >99%, Aladdin Reagent Co., Ltd., Shanghai, China) were weighed based on the chemical formula  $\text{Li}_{0.43}\text{Zn}_{0.27}\text{Ti}_{0.13}\text{Bi}_{0.003}\text{Fe}_{2.167}\text{O}_4$  (LiZnTiBi). Next, the weighed powders were blended by ball-milling method for 4 hours. In the process, the deionized water is selected as mixed media. The dried powders were pre-sintered at  $850^\circ\text{C}$  for 2 hours at  $\text{O}_2$  atmosphere to form spinel phase. According to molar ratio 0.43:0.27, the various  $\text{Li}_2\text{CO}_3$  and nano-ZnO (LZ) ( $x=0.00, 0.50, 0.75, 1.00$  and  $1.50 \text{ wt. } \%$ ) were added into the LiZnTiBi ferrite. Again, the mixtures were milled using planetary mill with a running speed of 250 rpm/min for 6 hours. After dried, the powders were granulated using PVA adhesive. And then, these particles were pressed into toroidal samples at  $\sim 10 \text{ MPa}$ . At last, the samples were sintered at  $875^\circ\text{C}$ ,  $900^\circ\text{C}$ , and  $925^\circ\text{C}$ , respectively.

### 2.2. Characterization

XRD peaks of LiZnTiBi ferrites with various  $\text{Li}_2\text{CO}_3$  and ZnO nanoparticles were measured by X-ray diffractometer (Cu  $\text{K}\alpha$  radiation, Rigaku, Japan). Scanning electron microscopy (SEM) images of the ferrites sintered at  $900^\circ\text{C}$  were measured using a scanning electron microscope (SEM, Q-45, and FEI). Saturation magnetization ( $M_s$ ) of the ferrites was measured by vibrating sample magnetometer (VSM) with  $\pm 5000 \text{ Oe}$  magnetic field. Volume densities of sintered

samples were measured by the Archimedes method in distilled water. The density of samples can be calculated by the formula:

$$\rho = \frac{m_0 \rho_0}{m_1 - m_2} \quad (1)$$

where  $m_0$  is weighing mass of samples in the air. After filling the gap in the samples with distilled water, the mass was weighed again, marked  $m_1$ . The  $m_2$  is mass of samples in the water. The saturation flux density ( $B_s$ ), remanence ( $B_r$ ), and coercivity force ( $H_c$ ) of the samples were tested with an Iwatsu BH analyzer (SY8232) in an alternating field 1600 A/m at 1 kHz. And all the tests were carried out under room temperature.

### 2.3. Results and Discussions

The XRD patterns of the LiZnTiBi ferrite with different LZ additives sintered at  $900^\circ\text{C}$  are shown in Figure 1. In the Figure 1, for all the samples, a pure spinel phase is observed. And all diffraction peaks, including (220), (311), (222), (400), (422), (511), (440), (620), (533), (622) and (444), are marked in the figure. The results indicated that adding a small quantity of  $\text{Li}_2\text{CO}_3$  and ZnO has no influence on formation of spinel phase polycrystalline LiZnTiBi ferrites at this calcination temperature ( $\sim 900^\circ\text{C}$ ). The result was consistent with the previous studied [18].

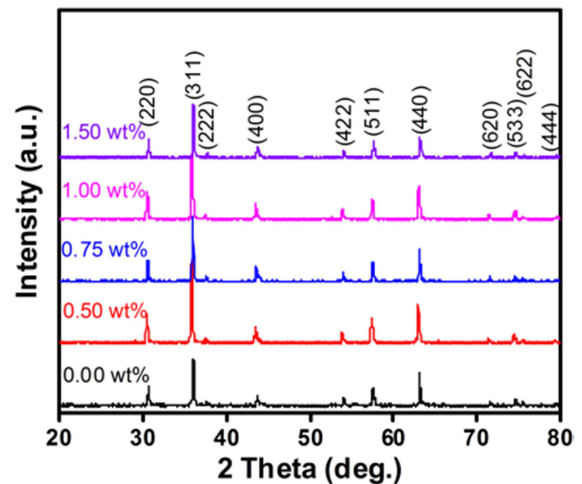


Figure 1. XRD patterns for LZ doped LiZnTiBi ferrites.

Microstructures of the LiZnTiBi ferrites with various LZ additives ( $x=0.50 \text{ wt}\% \sim 1.50 \text{ wt}\%$ ) are shown in Figure 2. In the Figure 2, all sample ferrites sintered at  $900^\circ\text{C}$  possess big average grain size (more than  $40 \mu\text{m}$ ). This can attributed to introduction of  $\text{Bi}_2\text{O}_3$ ,  $\text{Li}_2\text{CO}_3$  and nano-ZnO. In the Fig. 2a, when  $0.50 \text{ wt}\%$  LZ additives are added, there is some abnormal big grain ( $\sim 100 \mu\text{m}$ ). It can be explained by low activation energy and low-melting point  $\text{Li}_2\text{CO}_3$ . In addition, big grains resulted in appearance of small grains due to competitive relationship (Figure 2a). With more and more LZ additives are introduced, the LiZnTiBi ferrites possess uniform grains (see Figure 2c). This is due to increase of

ZnO nanoparticle, which can refine large grain. The phenomenon was similar with our previous work [18]. The moderate LZN nanoparticles can effectively control grain growth. However, when excess LZ additives are added, many small grains start to appear (in the Figure 2d) because of overmuch nano-ZnO. In a word, the moderate LZ additives can promote grain growth of LiZnTiBi ferrite sintered at low temperature.

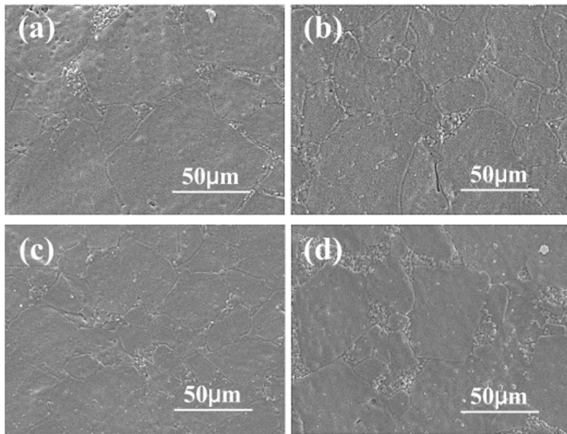


Figure 2. SEM images of LZ doped LiZnTiBi ferrites: (a) $x=0.50$  wt%, (b) $x=0.75$  wt%, (c) $x=1.00$  wt% and (d) $x=1.50$  wt%.

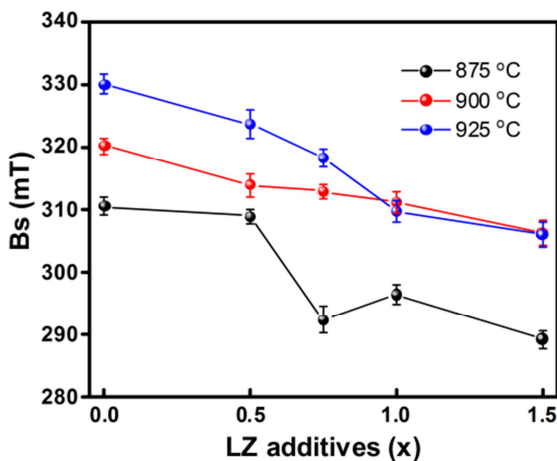


Figure 3. Saturation flux density ( $B_s$ ) of LiZnTiBi ferrites with various LZ additives sintered at different temperature.

Figure 3 show that saturation flux density ( $B_s$ ) of LZ doped LiZnTiBi ferrite sintered at different temperatures. It is apparent that the high sintering temperature can enhance  $B_s$  of the LiZnTiBi ferrite due to grain growth. When sintering temperature of samples is same, the ferrite sample with more LZ additives possesses low  $B_s$  value. However, the variation of  $B_s$  value is very small. For example, for ferrite samples sintered at 900°C, the value of  $B_s$  decrease from 320.2 mT to 306.2 mT, which is remain exceed 300 mT. The value was close to data reported by Liao et al. [19]. It was indicated that LZ is a selectable additive for the LiZnTiBi ferrite. The  $B_s$  value of samples sintered at 875°C have a large change when LZ additive more than 0.50 wt%, which can be explained by small grains (sintering temperature is too low). In a word,

because of introduce of LZ additive, the abnormal grain size can be controlled (see Figure 2c), the  $B_s$  of samples slightly reduced.

Figure 4 shows that remanence ratio ( $B_r/B_s$ ) of the ferrites. The change of  $B_r/B_s$  is opposite with  $B_s$  in the Figure 3, the samples sintered at 875°C have larger saturation flux density. However, in the Figure 4, the remanence ratio is smallest. In addition, the introduction of LZ additives leads to reduction of  $B_r/B_s$ . But for all samples, the  $B_r/B_s$  value is more than 0.83. The results indicated that the LZ doped LiZnTiBi ferrite possesses high remanence ratio.

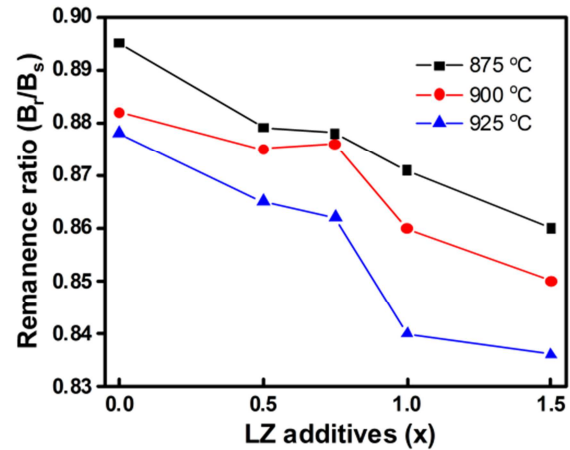


Figure 4. Remanence ratio ( $B_r/B_s$ ) of LZ doped LiZnTiBi ferrites.

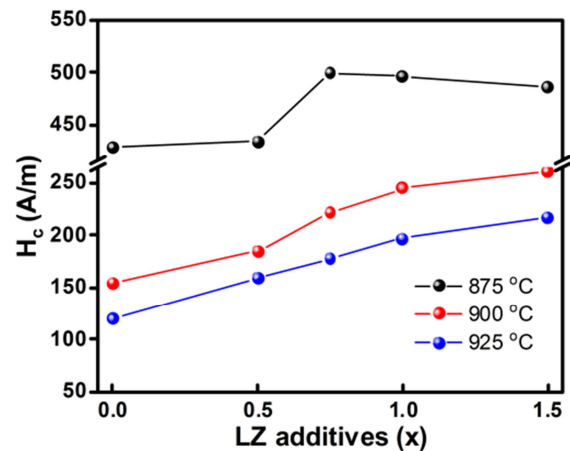


Figure 5. Changes of coercivity value of LZ doped LiZnTiBi ferrites.

The coercivity ( $H_c$ ) of LZ doped LiZnTiBi ferrite sintered at low temperatures are displayed in Figure 5. In general, the coercivity ( $H_c$ ) is inversely proportional to the grain size. Thus, in the Figure 5, the samples sintered at higher temperature have lower  $H_c$  value. Also, the change that  $H_c$  is consistent with grains size when various LZ additives were added. For the samples sintered at 875°C, the  $H_c$  value more than 400 A/m. The result is due to small grains. When sintering temperature more than 900°C, the  $H_c$  value obviously decreased.

The saturation magnetization of LZ doped LiZnTiBi ferrite sintered at 900°C is shown in Figure 6. In the Figure 6, all ferrite samples have similar magnetization curve. When

external magnetic field exceeds 2500 Oe, the samples are close to saturated state. The values of M<sub>s</sub> are listed in Table 1. With the increase of LZ additives, the value of M<sub>s</sub> gradually decreases. However, all samples have a high saturation magnetization (M<sub>s</sub> >70 emu/g). Thus, adding LZ additives has a little influence on saturation magnetization of LiZnTiBi ferrite.

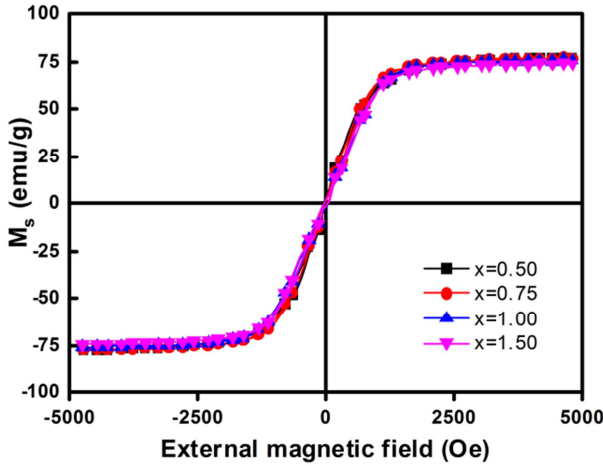


Figure 6. Saturation magnetization (M<sub>s</sub>) of different LZ doped LiZnTiBi ferrite ceramics sintered at 900°C.

Figure 7 shows that density of the LZ doped LiZnTiBi ferrite sintered at different temperatures. As shown in Figure 7, high sintering temperature can improve density of the LiZnTiBi ferrite samples due to enhance of grain growth and reduction of pores. In addition, when the ferrite samples were sintered at same temperature, the density of sample start to increased and then decreased. The phenomenon that improved density can be attributed to reduction of abnormal grains and densification. However, due to lower density of LZ composite additives, the density of ferrite samples started to reduce when more LZ additives were added. At last, when 0.75 wt% LZ additives were added, the ferrite possessed highest density at every sintering temperature.

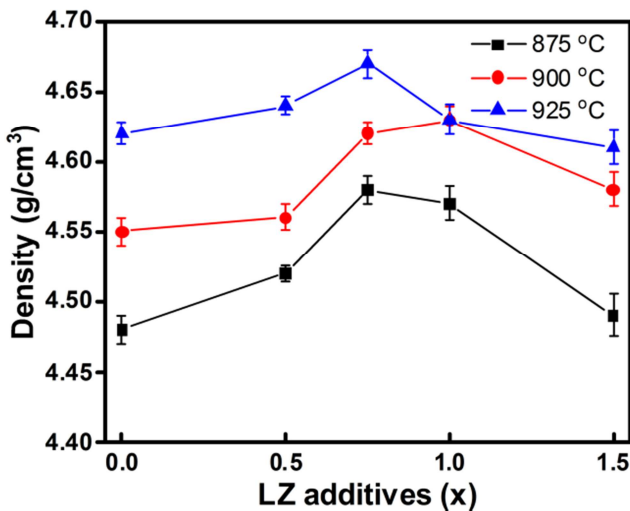


Figure 7. Density of different LZ doped LiZnTiBi ferrite ceramics sintered at different sintering temperatures.

Table 1 show important parameters of the LZ doped LiZnTiBi ferrite sintered at 900°C. The data of the table indicated that the LiZnTiBi ferrite with 1.00 wt% possesses high saturation flux density (B<sub>s</sub>=311.1mT), high remanence ratio (B<sub>r</sub>/B<sub>s</sub>=0.86) and low coercivity (H<sub>c</sub>=244.6 A/m). Moreover, the SEM image show the sample possesses uniform and compact grains.

Table 1. Important parameters of LZ doped LiZnTiBi ferrite sintered at 900°C.

LZ (wt%)	B <sub>s</sub>	B <sub>r</sub> /B <sub>s</sub>	H <sub>c</sub>	Density (g/cm <sup>3</sup> )	M <sub>s</sub> (emu/g)
0.00	320.2	0.88	154.6	4.55	78.64
0.50	313.9	0.87	185.2	4.56	76.74
0.75	312.9	0.87	221.3	4.62	76.72
1.00	311.1	0.86	244.6	4.63	75.40
1.50	306.2	0.85	260.5	4.58	73.79

### 3. Conclusion

In this work, low-melting point Li<sub>2</sub>CO<sub>3</sub> and nano-ZnO were selected as a new composite additive (LZ), which was added to LiZnTiBi (Li<sub>0.43</sub>Zn<sub>0.27</sub>Ti<sub>0.13</sub>Bi<sub>0.003</sub>Fe<sub>2.167</sub>O<sub>4</sub>) ferrite ceramic to promote solid-phase reaction at low temperature. Results, including saturation flux density (B<sub>s</sub>), remanence ratio (B<sub>r</sub>/B<sub>s</sub>) and saturation magnetization (M<sub>s</sub>) indicate that the LZ is a good additive. The magnetic properties of the LiZnTiBi ferrite ceramic have a weak deterioration. For example, the B<sub>s</sub> reduced from 320.2 mT to 311.1 mT when 1.00 wt% LZ was added. And the value of B<sub>r</sub>/B<sub>s</sub> reduced from 0.88 to 0.86. However, SEM image shows that the abnormal grains can be controlled by adding 1.00 wt% LZ additive. At last, a LiZnTiBi ferrite with great magnetic properties and uniform grains was obtained by using a new LZ additive when sintered at low temperature.

### Acknowledgements

This work was financially supported by Key Research and Development Projects of Sichuan Science and Technology Plan, No. 2019YFG0280. National Key Research and Development Plan (No. 2016YFA0300801), National Nature Science Foundation of China under Grant No. 61021061, and No. 61271037.

### References

- [1] A. Shamim, J. R. Bray, N. Hojjat, and L. Roy, “Ferrite LTCC-Based antennas for tunable SoP applications,” IEEE Trans. Comp. Pack. Man., 2011, vol. 1, pp. 999-1006.
- [2] E. Arabi, F. A. Ghaffar, and A. Shamim, “Tunable bandpass filter based on partially magnetized ferrite LTCC with embedded windings for SoP applications,” IEEE Micro. Wire. Comp. Lett., 2015, vol. 25, pp. 16-18.
- [3] F. A. Ghaffar and A. Shamim, “A partially magnetized ferrite LTCC-based SIW phase shifter for phased array applications,” IEEE Trans. Magn., 2015, vol. 51, pp. 271–350.

- [4] J. R. Bray, K. T. Kautio, and L. Roy, "Characterization of an experimental ferrite LTCC tape system for microwave and millimeter-wave applications," *IEEE Trans. Adv. Pack.*, vol. 27, pp. 558-565.
- [5] S. C. Yang, D. Vincent, J. R. Bray, and L. Roy, "Study of a ferrite LTCC multifunctional circulator with integrated winding," *IEEE Trans. Comp. Pack. Man.*, 2015, vol. 5, pp. 879-886.
- [6] E. Brookner, "Phased arrays and radars-Past, present and future," *Microwave J.*, 2006, vol. 49, pp. 24-46.
- [7] V. G. Harris, "Modern Microwave Ferrites," *IEEE Trans. Magn.* 2012, vol. 48, pp. 1075-1104.
- [8] F. Xu, Y. L. Liao, D. N. Zhang, T. C. Zhou, J. Lie, G. W. Gan, H. W. Zhang, "Synthesis of Highly Uniform and Compact Lithium Zinc Ferrite Ceramics via an Efficient Low Temperature Approach," *Inorg. Chem.*, 2017, vol. 56, pp. 4512-4520.
- [9] F. Xie, L. Jia, Z. Zheng, and H. Zhang, "Influences of  $\text{Li}_2\text{O-B}_2\text{O}_3\text{-SiO}_2$  Glass Addition on Microstructural and Magnetic Properties of  $\text{LiZnTi}$  Ferrites," *IEEE Trans. Magn.*, 2015, vol. 51, pp. 2801104.
- [10] T. C. Zhou, H. W. Zhang, L. J. Jia, J. Lie, Y. L. Liao, L. C. Jin, and H. Su, "Grain growth, densification, and gyromagnetic properties of  $\text{LiZnTi}$  ferrites with  $\text{H}_3\text{BO}_3\text{-Bi}_2\text{O}_3\text{-SiO}_2\text{-ZnO}$  glass addition," *J. Appl. Phys.*, 2014, vol. 115, pp. 17A511.
- [11] T. C. Zhou, H. W. Zhang, L. J. Jia, Y. L. Liao, Z. Y. Zhong, F. M. Bai, H. Su, J. Lie, L. C. Jin, and C. Liu, "Enhanced ferromagnetic properties of low temperature sintering  $\text{LiZnTi}$  ferrites with  $\text{Li}_2\text{O-B}_2\text{O}_3\text{-SiO}_2\text{-CaO-Al}_2\text{O}_3$  glass addition," *J. Alloy. Compd.*, 2015, vol. 620, pp. 421-426.
- [12] F. Xu, H. W. Zhang, F. Xie, Y. L. Liao, Y. X. Li, J. Lie, L. C. Jin, Y. Yang, G. W. Gan, G. Wang, and Q. Zhao, "Investigation of grain boundary diffusion and grain growth of lithium zinc ferrites with low activation energy," *J Am Ceram Soc.*, 2018, vol. 101, pp. 5037-5045.
- [13] D. Zhou, L. X. Pang, D. W. Wang, C. Li, B. B. Jin, and I. M. Reaney, "High permittivity and low loss microwave dielectrics suitable for 5G resonators and low temperature co-fired ceramic architecture," *J. Mater. Chem. C*, 2017, vol. 5, pp. 10094-10098.
- [14] M. T. Sebastian, and H. Jantunen, "Low loss dielectric materials for LTCC applications: a review," *Inter. Mater. Rev.* 2008, vol. 53, pp. 57-90.
- [15] S. Zhang, H. Su, H. W. Zhang, Y. L. Jing, and X. L. Tang, "Microwave dielectric properties of  $\text{CaWO}_4\text{-Li}_2\text{TiO}_3$  ceramics added with LBSCA glass for LTCC applications," *Ceram. Int.*, 2016, vol. 42, pp. 15242-15246.
- [16] Y. Wang, Y. L. Liu, J. Li, Q. Liu, H. W. Zhang, and V. G. Harris, "LTCC processed  $\text{CoTi}$  substituted M-type barium ferrite composite with BBSZ glass powder additives for microwave device applications," *AIP Adv.*, 2016, vol. 6, pp. 056410.
- [17] K. Lee, and S. Kang, " $\text{CuO/V}_2\text{O}_5$ -Codoped  $\text{Bi}_3/2\text{ZnNb}_3/2\text{O}_7$  (BZN) Ceramic for Embedded Capacitor Layer in Integrated LTCC Modules," *J. Electron. Mater.*, 2016, vol. 45, pp. 2987-2995.
- [18] F. Xu, D. N. Zhang, G. Wang, H. W. Zhang, Y. Yang, Y. L. Liao, L. C. Jin, Y. H. Rao, J. Lie, F. Xie, G. W. Gan, "Influence of LZN nanoparticles on microstructure and magnetic properties of bi-substituted  $\text{LiZnTi}$  low-sintering temperature ferrites," *Ceram. Int.*, 2019, vol. 45, pp. 1946-1949.
- [19] Y. L. Liao, H. Wang, D. N. Zhang, Y. X. Li, H. Su, J. Li, F. Xu, X. Y. Wang, H. W. Zhang, "Magnetic properties of low temperature sintered  $\text{LiZn}$  ferrites by using  $\text{Bi}_2\text{O}_3\text{-Li}_2\text{CO}_3\text{-CaO-SnO}_2\text{-B}_2\text{O}_3$  glass as sintering agent," *Ceram. Int.* 2018, vol. 44, pp. 5513-5517.